The finite-thickness effect is also found to be less significant at higher frequencies than at lower frequencies. This implies that the power is more densely confined to the dielectric under the strip as the frequency increases. Hence, the thickness of the strip has a smaller effect at higher frequencies. This inference will be made clear when the current distributions along the strip are presented.

B. Current Distributions

From the transverse magnetic field, the current density along the strip can be found. The longitudinal current distributions ($|I_z|/|I_z|_E$) around the strip are shown in Fig. 4(a). It is found that the currents along the $D-E$ contour become more dominant than those along the others as the frequency increases. That is, the higher the frequency, the more the transverse fields are confined to the substrate below the strip. This reflects the fact that the effective dielectric constant eventually tends to the dielectric constant of the substrate.

For the same cases as above, the transverse current distributions ($|I_t|/|I_t|_{\max}$) are shown in Fig. 4(b). On the whole, the increase in frequencies causes greater variations to the current distributions along the $B-C$ contour than those along the $C-D$ and $D-E$ contours. Especially at the higher frequency, the difference between the distributions at the corners C and D becomes more pronounced. In other words, the transverse current concentrates mainly near the corner D as the frequency increases.

IV. Conclusions

A full-wave analysis based on the variational conformal mapping technique to analyze the open microstrip line with finite strip thickness has been presented. Chang's mapping makes numerical analysis feasible. Numerical results are presented and are consistent with available data. The results provide the effective dielectric constants for the thicker strip. The numerical results also disclose that the longitudinal current distributions around the strip are confined to the substrate below the strip and that the transverse current distributions concentrate mainly toward the corner D as the frequency increases.

References

[1] R. A. Pucel, *Monolithic Microwave Integrated Circuits*. New York: IEEE, 1985.

[2] K. C. Gupta, R. Garg, and I. J. Bahl, *Microstrip Lines and Slotlines*. Dedham, MA: Artech House, 1979.

[3] P. Waldow and I. Wolff, "The skin-effect at high frequencies," *IEEE Trans. Microwave Theory Tech.*, vol. MTT-33, pp. 1076–1082, Oct. 1985.

[4] E. Yamashita and R. Mittra, "Variational method for the analysis of microstrip lines," *IEEE Trans. Microwave Theory Tech.*, vol. MTT-16, pp. 251–256, Apr. 1968.

[5] H. A. Wheeler, "Transmission line properties of parallel strip separated by a dielectric sheet," *IEEE Trans. Microwave Theory Tech.*, vol. MTT-13, pp. 172–185, Mar 1965.

[6] W. H. Chang, "Analytical IC metal-line capacitance formulas," *IEEE Trans. Microwave Theory Tech.*, vol. MTT-24, pp. 608–611, Sept. 1976.

[7] T. Itoh and R. Mittra, "Spectral-domain approach for calculating the dispersion characteristics of microstrip lines," *IEEE Trans. Microwave Theory Tech.*, vol. MTT-21, pp. 496–498, July 1973.

[8] P. Daly, "Hybrid-mode analysis of microstrip by finite-element methods," *IEEE Trans. Microwave Theory Tech.*, vol. MTT-19, pp. 19–25, Jan. 1971.

[9] F. Bogelsack and I. Wolff, "Application of projection method to a mode-matching solution for microstrip lines with finite metallization thickness," *IEEE Trans Microwave Theory Tech.*, vol. MTT-35, pp. 918–921, Oct. 1987.

[10] T. C. Edwards, *Foundations for Microstrip Circuits Design*. New York: Wiley, 1981

[11] C. Shih, R. B Wu, S. K. Jeng, and C. H. Chen, "A full-wave analysis of microstrip lines by variational conformal mapping technique," *IEEE Trans. Microwave Theory Tech.*, vol. 36, pp. 576–581, Mar 1988.

An Improved Design of Systems Based on Three Coupled Microstrip Lines

NABIL A. EL-DEEB, SENIOR MEMBER, IEEE

***Abstract*—An improved design of systems based on three coupled microstrip lines is introduced. The improvement lies mainly in the use of equal-mode-impedance lines, which greatly facilitates the design of the system. The design parameters of such a system are introduced in a manner that allows a simple systematic design procedure. An experimental coupler is realized and its practical performance is in good agreement with the theory.**

I. Introduction

The use of multiple coupled line structures, including three-line structures, for various applications in communications and microwave engineering has been extensively studied in the literature (e.g. [1]–[10]). The majority of these studies concentrated on the analysis of three-line systems and few considered the design parameters. A general three-line system, where the three lines have different widths and separations, is the most difficult to design and therefore only its analysis is considered (e.g. [8]). Meanwhile symmetrical three-line systems are found to be interesting in several applications (e.g. [1], [4], [5], [6]). Three equal-width coupled lines ($W_2 = W_1$, Fig. 1) are found to have five modal impedances, four of which are independent [9]. The line impedance for a given mode can be defined as the ratio of the voltage on a line to ground divided by the line current when the lines are propagating that mode. If the impedances of the three lines are equal when considering each mode separately there will be only three modal impedances and the system can be called an equal-mode-impedance system. This greatly facilitates the design of three-line systems. The equality of mode impedances is achieved by an appropriate increase of the width of the middle line (W_2) relative to that of the outer lines (W_1, see Fig. 1). The ratio (W_2/W_1) to achieve this equality has been determined for various combinations of geometrical dimensions of the three-line system on an alumina substrate ($\epsilon_r = 9.8$) [9].

In this paper the design parameters for a system of equal-mode-impedance lines are introduced in a manner that allow a simple systematic design of components. The design procedure is illustrated by designing a coupler to satisfy certain conditions, and the results agree well with the theory. Although the substrate material being considered is alumina, the procedure is applicable to other substrate materials (e.g. Teflon ($\epsilon_r = 2.2$) and quartz ($\epsilon_r = 3.78$)).

Manuscript received April 29, 1988; revised November 18, 1988
The author is with the Department of Electrical Engineering, Military Tech. College, Cairo, Egypt.
IEEE Log Number 8826055.

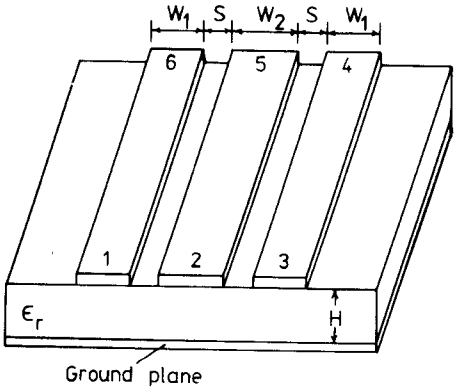

Fig. 1. A system of equal-mode-impedance microstrip lines

II. Design Parameters

For a system of three coupled equal-mode-impedance microstrip lines there are three propagating modes, which will be called modes A, B, and C. The design parameters are the mode impedances (Z_A, Z_B, and Z_C), the effective dielectric constants ($\epsilon_{eA}, \epsilon_{eB}, \epsilon_{eC}$), and the mode numbers (R_{2A}, R_{2B}, R_{2C}). These parameters, which are defined in [9], are computed and plotted for various geometrical dimensions of a system on an alumina substrate ($\epsilon_r = 9.8$, $H = 0.635$ mm). Since the expressions for the scattering parameters of [5] will be implemented here, the notations of [5] are used and matched with those of [9]. Modes A, B, and C in [9] correspond to modes B, C, and A in [5], respectively. Also, R_{2A}, R_{2B}, and R_{2C} in [9] correspond to m_1, m_2, and 0 in [5], respectively. Consequently Fig. 2 represents a plot of Z_B versus Z_C with W_1/H and S/H (Fig. 1) as parameters and is the first of the design curves. Then the rest of the design curves can be obtained from those presented in [9] by considering the aforementioned change in notations and excluding the dotted line curves corresponding to the equal-width system. The required curves of [9] presented in the appropriate sequence are fig. 7 (now representing variation of Z_A with geometrical dimensions), fig. 10 (now representing variation of m_1 with geometrical dimensions), fig. 5 (where $W_1 = W_3$), and fig. 11.This set of curves in the presented sequence allows a simple systematic design procedure, as explained by the following examples.

III. Design Examples

For a system of equal-mode-impedance lines there are three physically realizable configurations [5], two of which are of practical interest:

1) matching at side ports (ports 1, 3, 4, and 6) and isolation between ports 1 and 5, 3 and 5, 2 and 6, and 2 and 4 (Fig. 1);
2) matching at side ports (ports 1, 3, 4, and 6) and isolation between ports 1 and 3 and ports 4 and 6 (Fig. 1).

The design procedure to satisfy the requirements of the first configuration will be considered in detail since it will be used to realize an experimental coupler. The procedure to attain the second configuration will be outlined only briefly.

A. The First Configuration

From the expressions for the scattering parameters of an equal-mode-impedance system [5], we should have $T_B = T_C$ to have isolation between ports 1 and 5, 3 and 5, 2 and 6, and 2 and 4. T_B and T_C are the transmission coefficients for each of the lines for modes B and C, respectively, and are expressed in [5]. Under a quasi-TEM assumption and at the center frequency where the electrical length of the lines $\theta = 90°$, this condition together with matching at the side ports ($S_{11} = S_{33} = S_{44} = S_{66} = 0$) leads to

$$Z_B Z_C = Z_0^2 \tag{1}$$

$$\Gamma_B = -\Gamma_C \tag{2}$$

$$\Gamma_A = \frac{(m_1^2 - 2)}{(m_1^2 + 2)} \Gamma_B. \tag{3}$$

Z_0 is the terminating impedance at both ends of each of the lines (usually 50 Ω) [5]. Γ_A, Γ_B, and Γ_C are the reflection coefficients for each of the lines for modes A, B, and C, respectively, and are expressed in [5]. While m_1 (R_{2A} [9]) is the mode number for mode A for the middle line and is derived in [9], (1) is satisfied by the values lying on the dotted curve of Fig. 2, which represents this equation for $Z_0 = 50$ Ω. The design procedure then proceeds as follows.

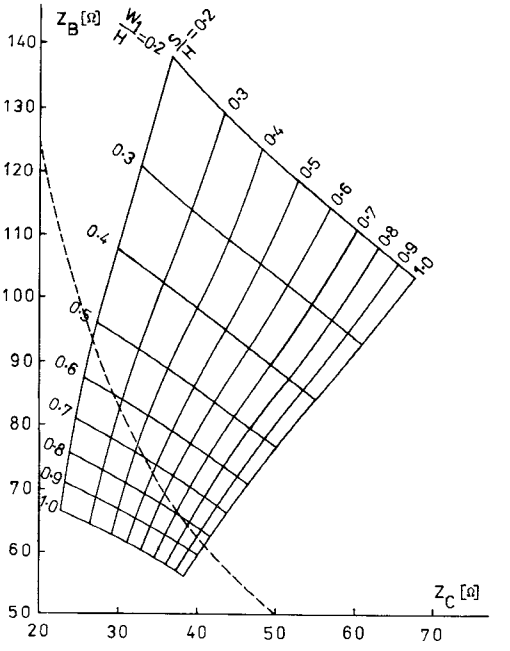

Fig. 2. Mode-B (Z_B) versus mode-C (Z_C) impedance with W_1/H and S/H as parameters

As a starting value m_1 is taken as 1, which is a reasonable choice, as can be seen from [9, fig. 10] ($m_1 = R_{2A}$ [9]). The required coupling between ports 1 and 2 in Fig. 1 (say, $S_{21} =$ 10 dB) can be used to determine the value of Z_B ($= 83.74$ Ω) by using the relation [5]

$$S_{21} = \frac{2m_1}{m_1^2 + 2} \Gamma_B. \tag{4}$$

The corresponding value of Z_C ($= 29.85$ Ω) can be determined from (1) or from Fig. 2. The corresponding geometrical dimensions W_1/H ($= 0.608$) and S/H ($= 0.28$) are determined from Fig. 2. When these dimensions are entered into [9, fig. 7] the value of Z_A ($= Z_C$ [9]) can be found ($= 47.75$ Ω). The corresponding value of m_1 can be determined from [9, fig. 10] ($= R_{2A} = 1.103$). When this value of m_1 is substituted into (4) a new value of Z_B ($= 82.33$ Ω) is obtained. From Fig. 2 the corresponding value of Z_C ($= 30.36$ Ω) and new values for W_1/H ($= 0.615$)

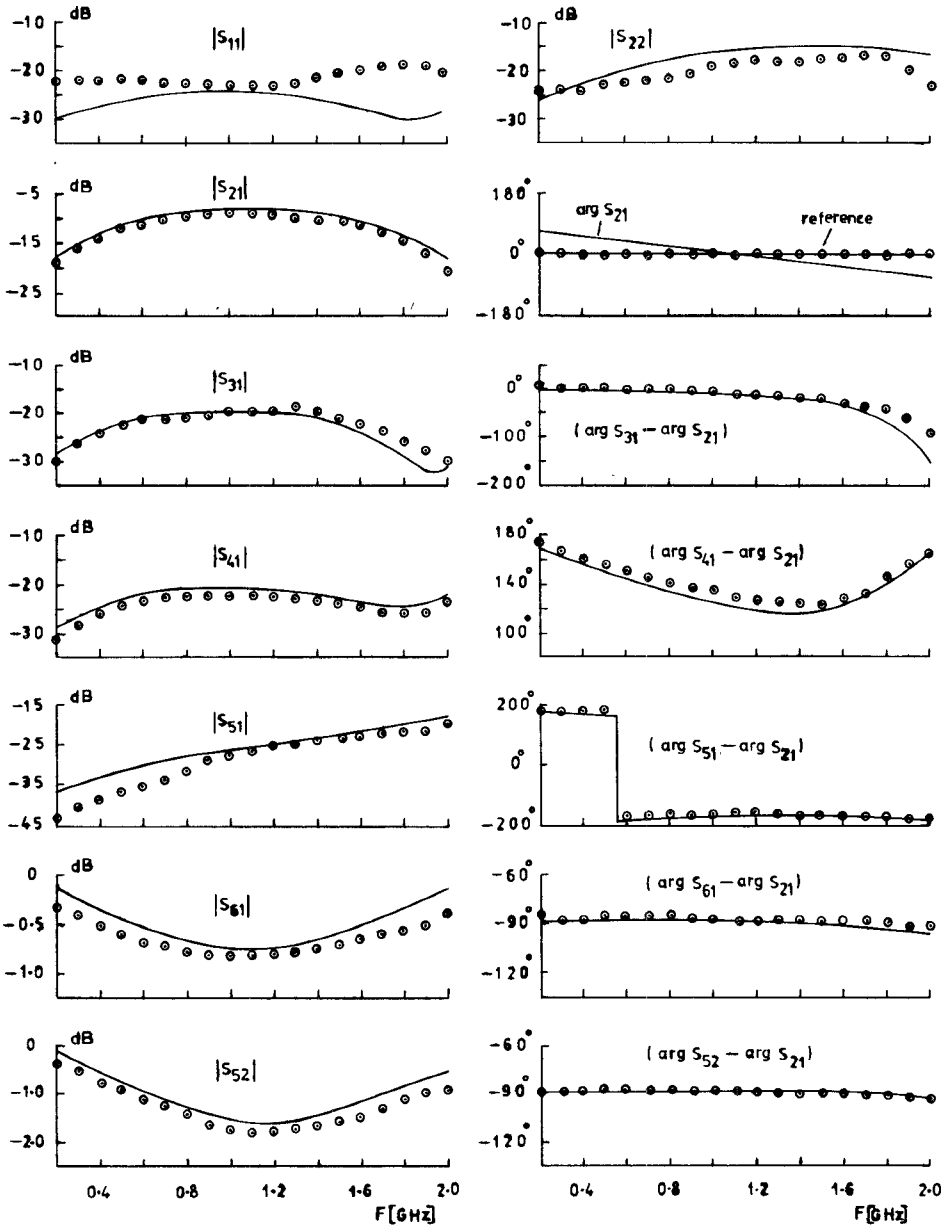

Fig. 3. Comparison of the theoretical (———) and practical (∘ ∘ ∘) behavior of the experimental coupler.

and S/H (= 0.31) can be obtained. When these new dimensions are entered into [9, fig. 7] a new value of Z_A is obtained (= 48.0 Ω). From [9, fig. 10] a new value of m_1 can be determined (= 1.105), which when substituted into (4) yields a second new value of Z_B (= 82.31 Ω). At this instant one iteration is finished and a second one can be started in the same sequence. After very few iterations (three for the present example) consistency is obtained (the corresponding parameters are $Z_B = 82.312$ Ω, $Z_C =$ 30.37 Ω, $W_1/H = 0.614$, $S/H = 0.309$, $m_1 = 1.1046$, and $Z_A =$ 47.95 Ω). When the final values of m_1 and Z_B are substituted into (3) a small discrepancy is found in the value of Z_A (= 44.7 Ω). This discrepancy, which can be attributed to the limited accuracy of obtaining data from the curves, is ineffective as compared with fabrication tolerances. Then the value of the width of the middle line (W_2) can be obtained from [9, fig. 5] ($W_2/W_1 = 1.306$). Finally the effective dielectric constant can be obtained from [9, fig. 11] ($\epsilon_{eA} = 5.755$, $\epsilon_{eB} = 7.155$, and $\epsilon_{eC} =$ 5.455). For a $\lambda/4$ coupler the length, at the chosen center frequency, can be determined from the relation [1]

$$L = 1/4(\lambda_A \lambda_B \lambda_C)^{1/3} \tag{5}$$

where

$$\lambda_A = \lambda_0/\sqrt{\epsilon_{eA}} \qquad \lambda_B = \lambda_0/\sqrt{\epsilon_{eB}} \qquad \lambda_C = \lambda_0/\sqrt{\epsilon_{eC}}$$

and λ_0 is the free-space wavelength at the center frequency.

B. The Second Configuration

From the scattering parameters of [5] we should have $\Gamma_A = 0$ and $\Gamma_B = -(m_1^2/2)\Gamma_C$. This leads, under the quasi-TEM assumption and at the center frequency, to the relations

$$Z_A = A_0 \tag{6}$$

$$Z_B^2 Z_C^2 = Z_0^4 \left(1 - \frac{(Z_B^2 - Z_C^2)(2 - m_1^2)}{Z_0^2(2 + m_1^2)}\right). \tag{7}$$

Since we have $Z_B > Z_C$ and $m_1^2 < 2$ ($\equiv Z_A > Z_B$ and $R_{2A}^2 < 2$ in

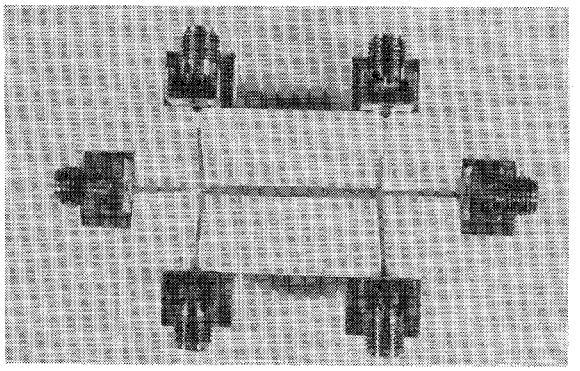

(a)

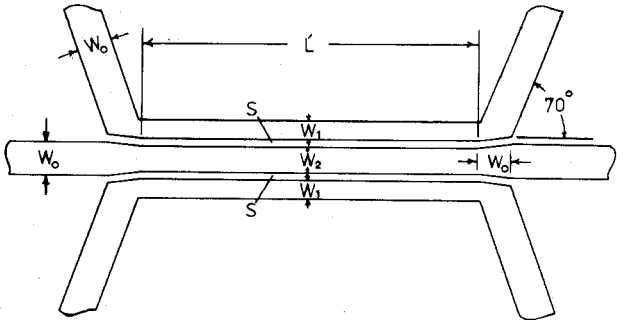

W_0=0·6 mm, W_1=0·334 mm, W_2=0·462 mm, S=0·13 mm

L=L'+W_0=26·63 mm (Substrate dimensions:50·8×25·4×0·635 mm)

(b)

Fig. 4. (a) Photograph of the experimental coupler. (b) The geometrical configuration of the experimental coupler.

[9]) equation (7) is satisfied for values of $Z_B A_C < Z_0^2$, shown as the area of Fig. 2 below the dotted curve. Here, also, we start with $m_1 = 1$ and from the required coupling between ports 1 and 2 (S_{21}) [5] and the condition $\Gamma_B = -(m_1^2/2)\Gamma_C$, the following relation can be obtained:

$$S_{21} = \frac{m_1}{(m_1^2+2)}(\Gamma_B - \Gamma_C) = \frac{1}{m_1}\Gamma_B. \tag{8}$$

Starting with $m_1 = 1$, as before, Z_B can be determined from (8) and then, consequently, Z_C. From Z_B, Z_C, and Fig. 2, the corresponding geometrical dimensions (W_1/H and S/H) can be determined. Then Z_A can be determined from [9, fig. 7] ($Z_A = Z_C$ [9]). Following an iteration sequence similar to that used for the first configuration we can arrive at the final values of the design parameters. The length of a $\lambda/4$ coupler satisfying the present conditions can be determined from (5).

Although the design parameters are obtained on a quasi-static basis, the effect of frequency can be accounted for by using a recently introduced dispersion model for three coupled microstrip lines [10].

To verify the design procedure a coupler is designed to satisfy the requirements of the first configuration. It was found experimentally, by cut and try technique, that to have a practical coupling of 10 dB a tighter design value of 8.7 dB is required. One possible explanation is the undercutting effect of the etching process used to obtain the microstrip circuit from the coated substrate. This process causes the separation between lines to be slightly wider and their widths to be narrower than their design values. It is also possible that the quasi-TEM approximation is not accurate enough. The corresponding design parameters are $Z_A = 47.87\ \Omega$, $Z_B = 91.66\ \Omega$, $Z_C = 27.77\ \Omega$, $m_1 = 1.058$, $\epsilon_{eA} = 5.645$, $\epsilon_{eB} = 7.035$, $\epsilon_{eC} = 5.435$, $W_1/H = 0.526$, $S/H = 0.206$, and $W_2/W_1 = 1.385$. A comparison between these latter parameters and the former ones gives an idea of the sensitivity of the electrical parameters, coupling, and consequently directivity to tolerances in the geometrical dimensions. The relative reduction in the separation between lines is larger than that in their widths to achieve tighter coupling. The corresponding relative increase in Z_B is almost equal to the relative decrease of Z_C (their product is theoretically constant). Smaller relative changes in the other parameters are observed.

The coupler can be designed at any center frequency of interest by determining its length L from (5). However, because of the available network analyzer (HP 8754 A, 8–2600 MHz) a center frequency of 1.15 GHz is chosen. This allows comparison of the practical and theoretical performances of the coupler, which is shown in Fig. 3, where good agreement is observed. A photograph of the experimental coupler and its geometrical configuration are shown in parts (a) and (b) of Fig. 4.

When designing the coupler at higher center frequencies (above 5 GHz) careful attention should be paid to the design of the transitions from the coupled lines to the 50 Ω lines (of width W_0 in Fig. 4(b)) leading to the measuring ports. This reduces the effect of reflections at these transitions on the coupler's behavior. The effect of dispersion starts to be appreciable as we approach 10 GHz and it can be considered by using the dispersion model of [10].

IV. Conclusions

The design parameters of three coupled equal-mode-impedance microstrip lines on an alumina substrate [9] are introduced in a manner that gives a convenient systematic design procedure. The design procedure for two configurations of this system is presented. A coupler satisfying the requirements of one of these configurations is realized and its practical performance is in good agreement with theory.The design procedure is applicable to any such system on any other isotropic substrate material. The design can be scaled to higher center frequencies and the effect of dispersion can be considered by using the mentioned dispersion model.

References

[1] D. Pavlidis and H. L. Hartnagel, "The design and performance of three-line microstrip couplers," *IEEE Trans. Microwave Theory Tech.*, vol. MTT-24, pp. 631–640, Oct. 1976.

[2] V. K. Tripathi, "On the analysis of symmetrical three-line microstrip circuits," *IEEE Trans. Microwave Theory Tech.*, vol. MTT-25, pp. 726–729, Sept. 1977.

[3] Y. Tajima and S. Kamihashi, "Multiconductor couplers," *IEEE Trans. Microwave Theory Tech.* vol. MTT-26, pp. 795–801, Oct. 1978.

[4] V. Tulaja *et al.*, "An interdigitated 3-dB coupler with three strips," *IEEE Trans. Microwave Theory Tech.*, vol. MTT-26, pp. 643–645, Sept. 1978.

[5] R. J. Collier and N. A. El-Deeb, "On the use of a microstrip three-line system as a six-port reflectometer," *IEEE Trans. Microwave Theory Tech.*, vol. MTT-27, pp. 847–853, Oct. 1979.

[6] R. J. Collier and N. A. El-Deeb, "Microstrip coupler suitable for use as a 6-port reflectometer," *Proc. Inst. Elec. Eng.*, pt. H, vol. 127, no. 2, pp. 87–91, Apr. 1980.

[7] V. K. Tripathi, "The scattering parameters and directional coupler analysis of characteristically terminated three-line structures in an inhomogeneous medium," *IEEE Trans. Microwave Theory Tech.*, vol. MTT-29, pp. 22–26, Jan. 1981.

[8] B. J. Janiczak, "Phase constant characteristics of generalized asymmetric three-coupled microstrip lines," *Proc. Inst. Elec.Eng.*, pt. H, vol. 132, no. 1, pp. 23–26, Feb. 1985.

[9] E. A. F. Abdallah and N. A. El-Deeb, "On the analysis and design of three coupled microstrip lines," *IEEE Trans. Microwave Theory Tech.*, vol. MTT-33, pp. 1217–1222, Nov. 1985.

[10] V. K. Tripathi, "A dispersion model for coupled microstrips," *IEEE Trans. Microwave Theory Tech.*, vol. MTT-34, pp. 66–71, Jan. 1986.